Jurnal Teknologi

Full paper

The Investigation on Size Reduction Feasibility of Planar Witricity Device for Biomedical Implantable Application

Mohd Hidir Mohd Salleh, Norhudah Seman*

Wireless Communication Centre , Universiti Teknologi Malaysia, 81310 UTM Johor Bahru, Johor, Malaysia

Corresponding author: huda@fke.utm.my

Article history

Received : 25 March 2015
Received in revised form : 11 April 2015
Accepted : 13 April 2015

Graphical abstract

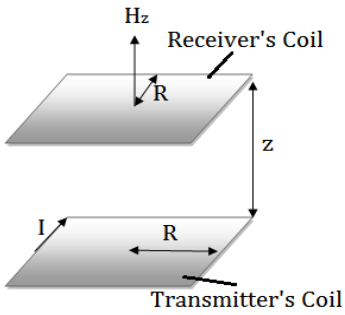

Abstract

This article presents the investigation on size reduction feasibility of planar Witricity device for biomedical implantable application. Biomedical implantable application demands for very small size device. Thus, the planar type of Witricity device is designed and investigated with the aim of size reduction. There are two designs presented in this article. Design A has larger size with an area dimension of 120 × 120 mm^2 and capable for energy transferable distance of 50 mm. Meanwhile, another Witricity device, namely Design B has smaller size of 80 × 80 mm^2 area is specified for approximately 40 mm transfer distance. The feasibility investigation on size reduction is observed from three main parameters; current distribution, coupling efficiency and return loss. The size reduction of 55% by Design B may lead to the reduction of 20% transfer distance but still with acceptable of 58% coupling efficiency at 40 mm that beneficial for biomedical applications.

Keywords: Magnetic resonance coupling; size reduction; wireless energy transfer; witricity

Abstrak

Artikel ini membentangkan kajian terhadap kebolehlaksanaan pengurangan saiz peranti satah *Witricity* untuk aplikasi implan bioperubatan. Aplikasi implan bioperubatan mempunyai permintaan terhadap peranti yang bersaiz sangat kecil. Oleh itu, peranti *Witricity* jenis satah direka dan dikaji dengan tujuan pengurangan saiz. Terdapat dua reka bentuk yang dikemukakan dalam artikel ini. Rekabentuk A mempunyai saiz yang lebih besar dengan satu dimensi berkeluasan 120 × 120 mm^2 dan mampu mencapai 50 mm jarak perpindahan tenaga. Sementara itu, peranti *Witricity* lain iaitu Rekabentuk B mempunyai saiz yang lebih kecil dengan keluasan 80 × 80 mm^2 yang dikhususkan untuk jarak perpindahan kira-kira 40 mm. Siasatan mengenai kebolehsanaan pengurangan saiz diperhatikan dari tiga parameter utama; edaran arus, kecekapan gandingan dan kehilangan pulangan. Pengurangan saiz 55% oleh Rekabentuk B boleh membawa kepada pengurangan jarak pemindahan sebanyak 20% tetapi masih boleh diterima dengan 58% kecekapan gandingan pada jarak 40 mm yang bermanfaat untuk aplikasi bioperubatan.

Kata kunci: gandingan resonans bermagnetik; pengurangan saiz; pemindahan tenaga tanpa wayar; *witricity*

1.0 INTRODUCTION

Recently, the research in fifth generation (5G) wireless communication technology has rapidly grown by focusing on the device-to-device (D2D) communication as one of their features [1]. The target is to develop D2D technology that enables the device to transmit and receive data on their own with very little manpower assistant and operation. Therefore, the development the wireless electricity or also known as Witricity becomes more significant due to its ability to transfer energy independently and efficiently over a mid-range distance. Following the vision of 5G that connection is not limited to communication devices but to anything at anywhere and anytime, this Witricity device with the capability of contactless energy transfer seems to be promising to be applied in biomedical application.

Witricity, the abbreviation of wireless electricity is a specific technical term for wireless energy transfer (WET) using strongly coupled magnetic resonance technique [2-7]. This method was firstly convinced by a research team in Massachusetts Institute of Technology (MIT) in 2007 by lightning a 60 watts bulb with 40% efficiency and transfer distance of about two meters. WET using Witricity is a new technique developed from conventional inductive coupling with special conditions of operate at strong coupling regime, thus

provide modest transfer and dissipation loss to other resonant objects compared to all intrinsic loss rates [4]. The Witricity system illustrated in Figure 1, which based on near field coupling only allows the energy exchange to its resonant pair.

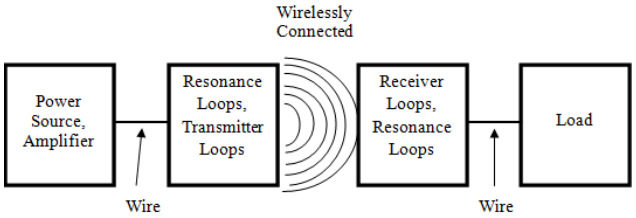

Figure 1 Basic configuration in Witricity device system [2]

Referring to Figure 1, the Witricity components include power source and amplifier connected to source resonance loop, the resonance loop is used to resonate the energy to the transmitter loop. The resonance loop for this work is designed on a single substrate together with the transmitter loop. Then, the energy is wirelessly sent to the receiver. At the receiver, the components involved are similar to the transmitter except the connection to the load instead of power source and amplifier.

The applications using Witricity device can be varied from large energy consumption based application such as electric vehicle [8-10], television and other electrical appliances to the small electronic devices such as laptop, mobile phone, electric tooth brush and many more.

In biomedical application, the development of Witricity is not less important as it has the feasibility to replace the procedure of a highly cost surgery to replace the battery of the implantable device. The implantable device is the device implanted in human body such as to monitor and diagnose the condition of the heart and brain. For example, deep-brain stimulation (DBS) device is implanted in the Parkinson's patient brain for treating and essential tremor [11]. Other implantable devices such as cochlear implants [12], retinal prosthesis [13] and pacemaker [14] also have been gaining global attention nowadays [15]. The implantable devices are commonly utilized a non-rechargeable high-capacity battery, which allows the long-term device operating times for up to several years [16-19]. When the energy stores in the battery have been depleted, a highly cost surgery needs to be done to replace the battery. The total cost for single replacement, including the devices, surgery and accessories are approximately USD 25 000 that probably make it one of the most expensive battery change in the world [17].

Hence, this article shows the feasibility in designing reduced-size Witricity device with investigation of three main parameters; current distribution, coupling efficiency and return loss performance. In achieving the goal of this investigation, two designs are presented, which different in size with concerned operating frequency of tens of MHz that less than 30 MHz. The design, optimization and analysis are conducted via the use of a full-wave electromagnetic simulation software package, CST Microwave Studio.

■2.0 WITRICITY THEORY

The most important features in the Witricity design are the transmitting and receiving coil. There are several types of coils that frequently used in designing Witricity device such as circular helical coil and spiral planar coil. The selection of the coil types is based on its application. In this article, the rectangular planar spiral coil type is chosen due to its thin size and has feasibility to be compact.

The Witricity device, which consists of transmitter and receiver, must be aligned horizontally or vertically to perform at optimum condition. The alignment of the transmitter and receiver can be shown in Figure 2. The center of the transmitter must be aligned to the center of the receiver. Any misalignment occurred either lateral or angular might result degradation to the performance of energy transfer. However, the device must be able to tolerate some degree of lateral and angular misalignment, which cannot be avoided practically.

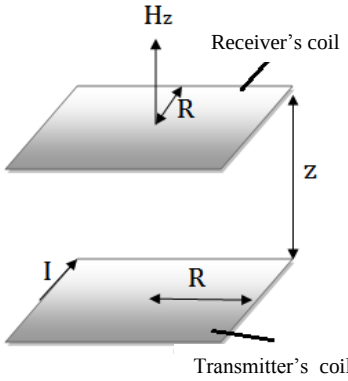

Figure 2 Magnetic field vector for transmitter and receiver of Witricity having *z* air gap

The amount of magnetic-field from the transmitter that experienced by the receiver can be derived from [20] as been shown by Equation (1);

$$Hz = \frac{I[R^2+z^2]^{1/2}}{2\pi}[K(m) + (R^2 - z^2)E(m)] \quad (1)$$

where, *I*, *R*, and *z* are the current flow through the coil, the average coil radius and air gap transfer distance, respectively. Meanwhile, *K*(*m*) and *E*(*m*) are the complete elliptical integral of the first and second kind, accordingly that can be expressed by Equation (2) and (3) [21];

$$K(m) = \int_0^{\pi/2} \frac{d\theta}{(1-m\sin\theta)^{1/2}} \quad (2)$$

$$E(m) = \int_0^{\pi/2} (1 - m\sin\theta)^{1/2}\, d\theta \quad (3)$$

where, *m* and θ are the parameter of elliptical integrals that sometimes used as k^2 and the complete elliptical angle, respectively. The value of complete elliptical angle, θ should between 0 and $\pi/2$.

The distance, z between the transmitter and receiver may be varied depending on the location of the battery that has been implants. However, the minimum distance of at least several mm must be kept, which imposes the implantation of a coil under the skin [22].

■3.0 WITRICITY DESIGN

Two Witricity devices are presented with different sizes that have the design layout of top and bottom layer as shown in

Figure 3. Design A has large size of 120 x 120 mm^2 of area dimension, while Design B has the smaller size of 80 x 80 mm^2. The top layer consists of the transmitting or receiving rectangular-shaped spiral coil with certain numbers of turns. Meanwhile, the bottom layer has four rectangular-shaped capacitor plates attached to a single loop of source/load coil. Both designs utilize FR4 substrate that has 1.6 mm thickness with double-sided copper clad, relative permittivity of 4.41, loss tangent of 0.025 and copper coating thickness of 0.035 mm.

A set of transmitter and receiver as depicted in Figure 4 has identical design to ensure they operate at exactly similar frequency. Where, different in size and dimension may result different resonant frequency and performance. In addition, the differences also occurred when the transmission distances are varied. The designs presented only consider tens of MHz of operating frequency, which less than 30 MHz. This is due to within this range, a very low propagation loss can be expected.

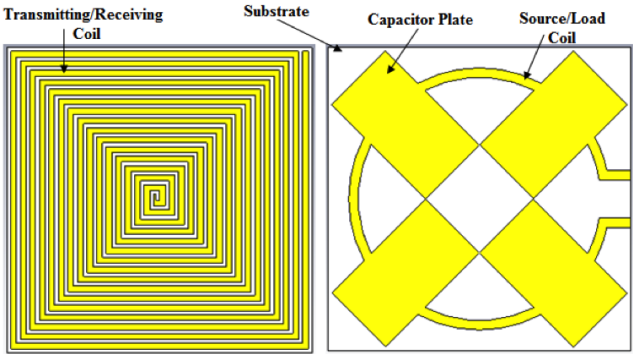

Figure 3 (a) Top and (b) bottom layout of the proposed planar Witricity device

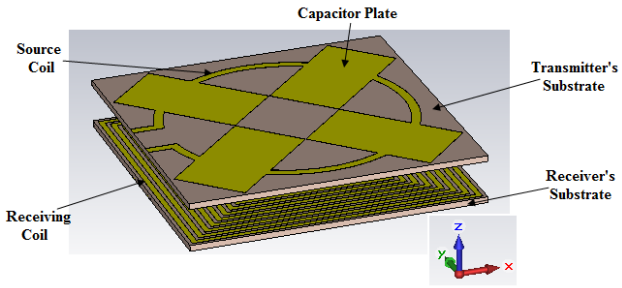

Figure 4 The three-dimensional (3D) CST generated layout that showing the alignment and air gap separation between the transmitter and receiver

Design A and B are designed and optimized via the use of CST Microwave Studio with concern of the best performance of coupling efficiency and return loss. The summary of the optimized dimensions of the designed Witricity device are shown in Figure 5.

Besides different in size, in order to operate within the designated operating frequency, Design A and B have distinctive optimized dimensions. Top layer of Design A consists of 8 turns of rectangular-shaped spiral coil with width of 5.675 mm and gap between each turn of 1.2 mm. Whilst, Design A's bottom layer has four rectangular-shaped capacitor plates and a coil with width of 2.5 mm. Each of its capacitor plate has a size of 23 × 52 mm^2. Meanwhile, Design B has a higher number of rectangular spiral coil turn, which is 16. Hence, its width and gap between each turn are thinner and narrower than Design A, respectively. The width of spiral coil is 1.5 mm, while its gap is 1 mm. Furthermore, Design B's bottom layer has a similar number of rectangular-shaped capacitor plates with size of 20 × 35 mm^2 and coil width of 2.5 mm.

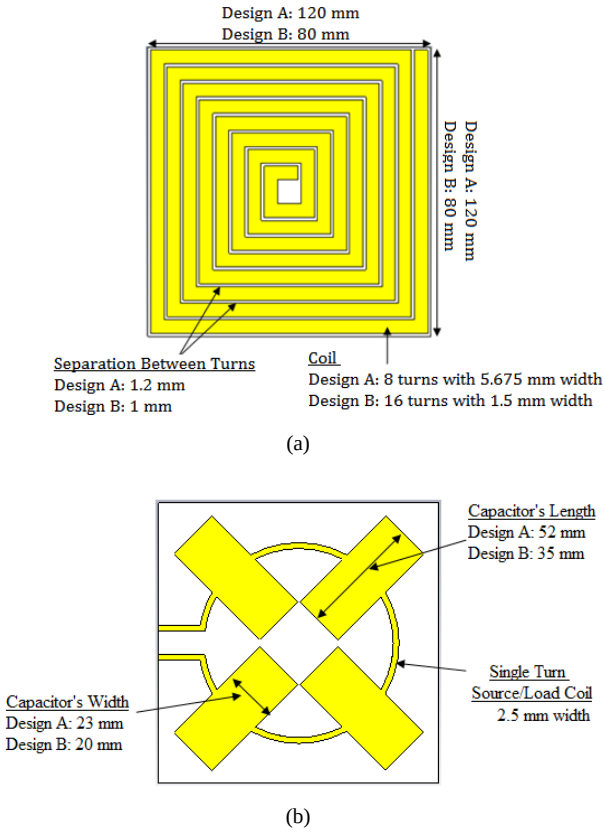

Figure 5 The optimized dimensions of the designed Witricity devices from (a) top and (b) bottom view

4.0 RESULTS AND DISCUSSION

The current distribution and S-parameter performances for Design A and B of Witricity devices are discussed in this section. The current distribution reflects the intensity of current during power transfer at certain location. Then, S-parameter investigation of both designs concerns the coupling efficiency and return loss, which are based on the transmission coefficient of S_{21} and reflection coefficient of S_{11}, respectively.

A. Current Distribution

The current distribution is investigated by fixing the distance between the transmitter and receiver to be at 10 mm, 30 mm and 50 mm which applied to both Design A and B as shown in Figure 6 and 7, respectively.

The simulated distribution of surface currents' distribution is presented with the legend indicates the intensity level of the respecting colour scheme. The highest and lowest current intensity are showing by red and dark blue, accordingly.

Referring to Figure 6, Design A shows greater current distribution intensity at 10 mm followed by 30 mm and 50 mm

transfer distance as expected. Where, largest area of highest intensity shown by red colour can be noted at 10 mm compared to at 30 mm and 50 mm. The differences between current distribution intensity at 10 mm, 30 mm and 50 mm are minimal. Hence, good coupling efficiency can be expected for all concerned distances up to 50 mm.

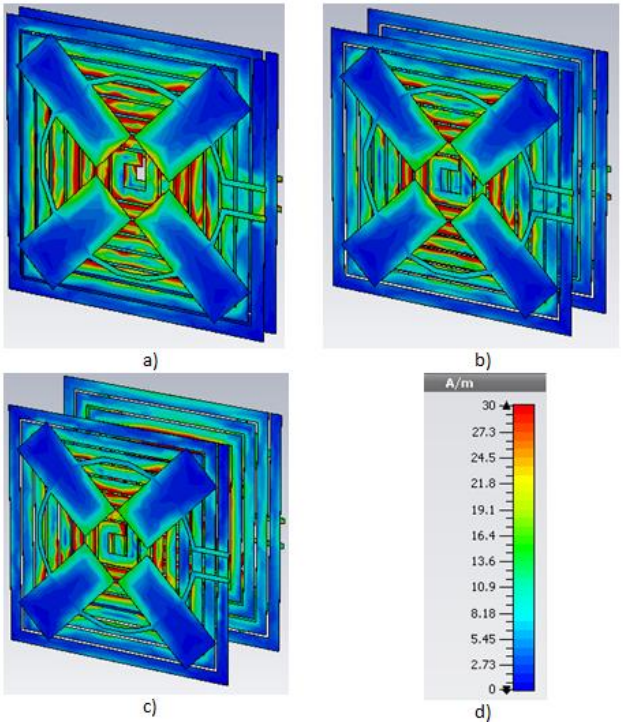

Figure 6 The current distribution for Design A at (a) 10 mm, (b) 30 mm and (c) 50 mm transfer distance with (d) its legend

Meanwhile, Figure 7 depicts the surface current distribution of Design B. The difference level of intensity can be clearly seen between three varied distances; 10 mm, 30 mm and 50 mm. The highest surface current intensity shown at 10 mm, where it has current distribution value of about 20-30 dB that can be noted being concentrated at its middle area. While, at the edge of the design, quite low current distribution can be seen, with approximately 5 to 10 dB. Meanwhile, Design B at 30 mm distance demonstrates slightly lower current distribution compared to 10 mm but still with a convincing level of current distribution concentrated at the center. However, moderate current distribution can be seen at 50 mm distance due to farther transfer distance between the transmitter and receiver.

Hence, referring to the depicted simulated current distribution, the more consistent current distribution intensity is expected to offer better coupling efficiency. Thus, Design A can be assumed to have good coupling efficiency for all varied distances and better transferable distance than Design B. However, this does not warrant worst performance from Design B.

B. S-Parameters

Figure 8 shows the coupling efficiency, η_{21} of the Design A and B of Witricity devices. The coupling efficiency, η_{21} is computed from the transmission coefficient of S_{21} as expressed in the following Equation (4):

$$\eta_{21}(\%) = |S_{21}|^2 \times 100\% \quad (4)$$

Generally, Design A demonstrates higher coupling coefficient compared to Design B as predicted from the observation made on the current distribution performance, when the distance between transmitter and receiver is varied from 10 mm to 50 mm.

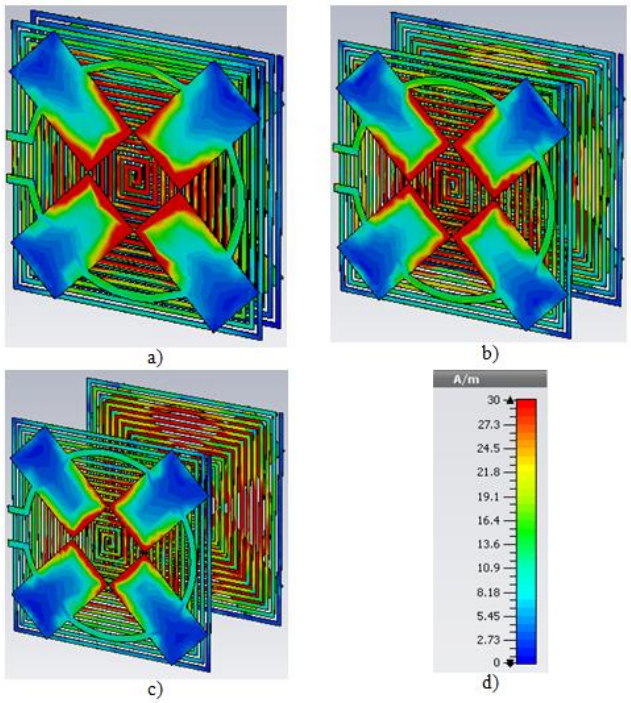

Figure 7 The current distribution for Design B at (a) 10 mm, (b) 30 mm and (c) 50 mm transfer distance with (d) its legend

The Design A's coupling efficiency is slightly decreasing from 75% to 72% that inversely proportional to the increment of the transfer distance from 10 mm to 40 mm. Even at 50 mm, 61% of coupling efficiency still can be achieved. Meanwhile, Design B has approximately ~70% coupling efficiency up to 30 mm transfer distance. At 40 mm, the efficiency degrades to 58%, which still can be considered good as in the wireless power transfer at least 50% efficiency is expected. The overall performances are compared in Table 1.

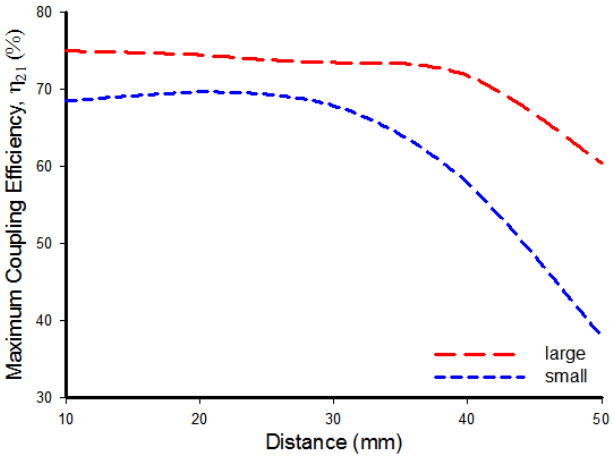

Figure 8 The maximum coupling efficiency of Design A and B that denoted by 'large' and 'small' in the legend for several varied transfer distances

The matching performances for both designs are evaluated from the reflection coefficient at the input port as plotted in Figure 9 and 10, which reflect their return losses. The plotted results show reflection coefficient, S_{11} from 10 to 50 mm transfer distance. Generally, since this device consists of the coupled transmitter and receiver, the size and varied distance will consequently, change the operating frequency as can be noted from the obtained results. The changes in operating frequency reflect the change of effective inductance and capacitance for overall design [2]. In particular, the capacitance is depending on the dimension of the conductor, the distance or the thickness of the coupling medium and the medium permittivity. As the distance of the coupling medium increases, which is air in this case, the capacitance is decreasing. Thus, resulting the increment of operating frequency that inversely proportional to the capacitance. Furthermore, at the same distance, lower performance can be observed for Design B. Where, the large size of Witricity shows good matching impedance up to 50 mm distance, while the smaller size result shows distortion at 50 mm. Considerable good matching of better than 10 dB still can be achieved by Design B up to 40 mm. The summarized performances for design A and B are listed in Table 1.

Referring to the plotted results and the summarized performances in Table 1, the advantages of having a large size of Witricity device are the capability of achieving farther transferable distance and good matching performance. However, by considering of the current demand of small and tiny device, this feasibility study is essential and has proven the possibility to design a smaller Witricity device that suitable for the biomedical implantable device. Based on the obtained results, it is worth having a transferable distance decrement of 20% from 50 mm to 40 mm as the design size can be reduced by 55.6% from 144 cm^2 to 64 cm^2. Where, this smaller size of Design B still offers an optimal coupling efficiency of 58% with a good return loss of 17.7 dB.

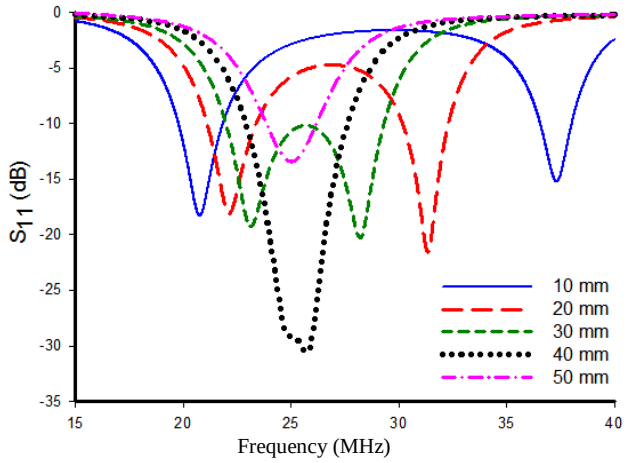

Figure 9 The performance of S_{11} of Design A from 10 mm to 50 mm transferable distance.

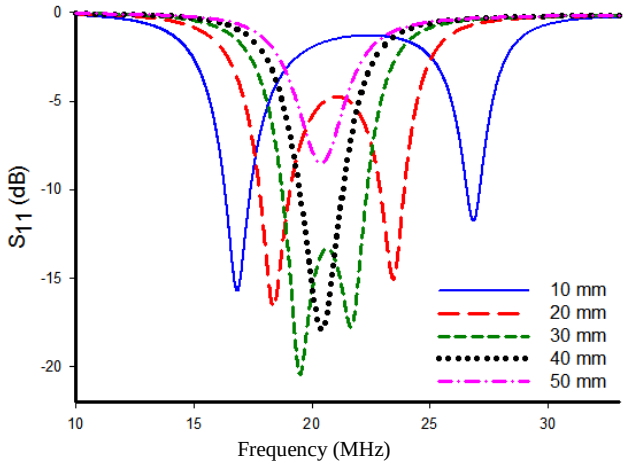

Figure 10 The performance of S_{11} of Design B from 10 mm to 50 mm transferable distance.

Table 1 Summarized performance of the designed witricity devices

Witricity Device	Distance (mm)	Parameters		
		Centre Frequency (MHz)	Coupling Efficiency (%)	Return Loss (dB)
Design A	10	20.8	75	18.3
	20	22.3	74	17.5
	30	23.5	73	17.4
	40	25.1	72	29.2
	50	24.9	61	13.3
Design B	10	16.8	68	15.5
	20	18.5	70	15.9
	30	19.8	68	17.6
	40	20.3	58	17.7
	50	20.2	38	8.3

5.0 CONLUSION

The investigation on size reduction feasibility of planar Witricity device has been presented in this article. Two designs have been shown, where Design A has dimension of 120 × 120 mm^2 and demonstrated a good energy transferable distance up to 50 mm. While, the smaller size of Witricity device, namely Design B with 80 × 80 mm^2 area has approximately up to 40 mm transfer distance. The 55% size reduction offered by Design B has 20% transferable distance reduction. However, it can be concluded that it is still capable to promise an acceptable of 58% coupling efficiency and good matching of 17.7 dB return loss at 40 mm transfer distance. Hence, this study has proven the feasibility in designing reduced-size Witricity device with good performance and transferable distance. The finding in this article will be used in the further research of the reduced-size Witricity device by using a thinner substrate with higher dielectric relative permittivity that might be very favorable to be used in biomedical application.

Acknowledgement

This work is carried out with the financial support from the Malaysian Ministry of Education (MOE) via Fundamental Research Grant Scheme (FRGS) with vote number of 4F206, MyPhD program and Universiti Teknologi Malaysia (UTM) via GUP Grant with vote number of 05H43.

References

[1] B. Bangerter, S.Talwar, R. Arefi, K. Stewart. 2014. Networks and Devices for the 5G Era. *IEEE Communications Magazine*. 52: 90–96.

[2] M.H. Salleh, N. Seman and R. Dewan. 2013. Reduced-size Witricity Charger Design And Its Parametric Study. IEEE International RF and Microwave Conference. 387–390.

[3] A. Kurs, A. Karalis, R. Moffatt, J. D. Joannopoulos, P. Fisher, M. Soljačić. 2007. Wireless Power Transfer Via Strongly Coupled Magnetic Resonances. *Science*. 317 (5834): 83–86 .

[4] A. Karalis, J.D. Joannopoulos, M. Soljačić. 2008. Efficient Wireless Non-Radiative Mid-range Energy Transfer. *Annals of Physics*. 323: 34–48.

[5] A. Karalis, A. Kurs, R. Moffatt, J. D. Joannopoulos, P. H.Fisher, M. Soljacic. 2010. United States Patent: Wireless Power Transfer, Patent no. US7825543B2.

[6] D.G.Nottiani and F.Leccese. 2012. A Simple Method for Calculating Lumped Parameters of Planar Spiral Coil for Wireless Energy Transfer. 11th International Conference on Environment and Electrical Engineering. 869-872.

[7] H. Zhou and S. Yang. 2012. Resonant Frequency Calculation of Witricity Using Equivalent Circuit Model Combined with Finite Element Method. Sixth International Conference on Electromagnetic Field Problems and Applications. 1–4.

[8] G. A. J. Elliott, J. T. Boys and A. W. Green. 1995. Magnetically Coupled Systems for Power Transfer to Electric Vehicles. in Proc. Int. Conf. Power Electron. Drive System. 797–801.

[9] S. Y. Hui, 2013. Planar Wireless Charging Technology for Portable Electronic Products and Qi. *Proceedings of the IEEE*. 101: 1290–1301.

[10] J. R. Severns, E. Yeow, G. Woody, J. Hall, and J. Hayes. 1996. An Ultra-Compact Transformer for a 100W to 120kW Inductive Coupler for Electric Vehicle Battery Charging. Proc. 11th Annual IEEE Applied Power Electronics Conference and Exposition. 1: 32–38.

[11] F. Zhang, S..A. Hackworth, X. Liu, H. Chen, R..J. Sclabassi, M. Sun. 2009. Wireless Energy Transfer Platform For Medical Sensors and Implantable Devices. Annual International Conference of the IEEE Engineering in Medicine and Biology Society. 1045–1048.

[12] J. Wang and K. D. Wise. 2008. A Hybrid Electrode Array with Built-In Position Sensors for an Implantable MEMS-Based Cochlear Prosthesis. *Journal of Microelectromechanical Systems*. 17: 1187–1194.

[13] L. Wen, D.C. Rodger, E. Meng, J.D. Weiland, M.S. Humayun, and T. Yuchong. 2008. Wafer-Level Parylene Packaging With Integrated RF Electronics for Wireless Retinal Prostheses. *Journal of Microelectromechanical Systems*. 19: 735–742.

[14] P. N. Gray, R. Tierney, X. Gray, and L. M. Treanor. 2006. eGanges Pervasive Peacemaker. 1st International Symposium on Pervasive Computing and Applications Urumqi. 433–438.

[15] Y. Li, X. Li; F. Peng, H. Zhang, W. Guo, W. Zhu, T. Yang. 2013. Wireless Energy Transfer System Based on High Q Flexible Planar-Litz MEMS Coils. 8th IEEE International Conference on Nano/Micro Engineered and Molecular Systems (NEMS). 837–840.

[16] M. Sun, G. A. Justin, P. A. Roche, J. Zhao, B. L. Wessel, Y. Zhang, R. J. Sclabassi. 2006. Passing Data And Supplying Power To Neural Implants. *IEEE Engineering in Medicine and Biology Magazine*. 25(5): 39–46.

[17] N. Yin, G. Xu, Q. Yang, J. Zhao, X. Yang, J. Jin, W. Fu, M. Sun. 2012. Analysis of Wireless Energy Transmission for Implantable Device Based on Coupled Magnetic Resonance. *IEEE Transactions on Magnetics*. 48(2): 723–726.

[18] S. Smith and R. Aasen. 1992. The Effects of Electromagnetic Fields on Cardiac Pacemakers. *IEEE Trans. Broadcast*. 2: 136–139.

[19] S. A. P. Haddad, R. P. M. Houben and W. A. Serdijn. 2006. The Evolution of Pacemakers. *IEEE Engineering in Medicine and Biology Magazine*. 25: 38–48.

[20] N. M. Quoc, P. Woods, S. Young-Sik, S. Rao, J. C. Chiao. 2013. Position and Angular Misalignment Analysis for A Wirelessly Powered Stimulator. IEEE MTT-S International Microwave Symposium Digest (IMS) 2013. 1(3): 2–7.

[21] R. H. Good. 2001. Elliptic Integrals, the Forgotten Functions. *European Journal of Physics*. 22: 119–126.

[22] S. Hached, A. Trigui, I. E. Khalloufi, M. Sawan. 2014. A Bluetooth-based Low-energy Qi-compliant Battery Charger for Implantable Medical Devices. 2014 IEEE International Symposium on Bioelectronics and Bioinformatics. 1–4.